The Journal of Experimental Biology 210, 1378-1390
Published by The Company of Biologists 2007
doi:10.1242/jeb.001545

Mechanics of cutting maneuvers by ostriches (*Struthio camelus*)

Devin L. Jindrich[1,*], Nicola C. Smith[2], Karin Jespers[2] and Alan M. Wilson[2,3]

[1]*Department of Kinesiology, Physical Education Building East 107B, Arizona State University, Tempe AZ, 85287-0404, USA,* [2]*Structure and Motion Laboratory, The Royal Veterinary College, Hawkshead Lane, North Mymms, Hatfield, Hertfordshire, AL9 7TA, UK and* [3]*Structure and Motion Laboratory, Institute of Orthopaedics and Musculoskeletal Sciences, University College London, Royal National Orthopedic Hospital, Brockley Hill, Stanmore, Middlesex, HA7 4LP, UK*

*Author for correspondence (e-mail: devin.jindrich@asu.edu)

Accepted 6 February 2007

Summary

We studied the strategies used by cursorial bipeds (ostriches) to maneuver during running. Eight ostriches were induced to run along a trackway and execute turns. Ground reaction forces and three-dimensional kinematics of the body and leg joints were simultaneously recorded, allowing calculation of joint angles and quasi-static net joint torques. Sidesteps, where the leg on the outside of the turn changes the movement direction, and crossovers using the inside leg, occurred with nearly equal frequency. Ostriches executed maneuvers using a simple control strategy that required minimal changes to leg kinematics or net torque production at individual joints. Although ostriches did use acceleration or braking forces to control body rotation, their morphology allowed for both crossovers and sidesteps to be accomplished with minimal net acceleratory/braking force production. Moreover, body roll and ab/adduction of the leg shifted the foot position away from the turn direction, reducing the acceleratory/braking forces required to prevent under- or over-rotation and aligning the leg with the ground reaction force.

Key words: sidestepping, cutting, maneuverability, stability, navigation, locomotion.

Introduction

Terrestrial animals that differ widely in mass, morphology and lineage can show similar locomotor mechanics (Full, 1989). For constant-average-speed terrestrial locomotion, animals resemble relatively simple 'spring-loaded inverted pendulum' (SLIP) systems (Cavagna et al., 1977; Farley et al., 1993). Using simple mathematical models such as the SLIP model to describe movement allows for design and function to be understood in terms of overall mechanical task constraints (Full and Koditschek, 1999). For example, considering human legs as linear springs allowed the joints most responsible for leg stiffness to be identified (Farley and Morgenroth, 1999).

In contrast to constant-average-speed locomotion, the mechanics of unsteady locomotion are poorly understood (Alexander, 2003; Dickinson et al., 2000; Greene, 1985). Greene and McMahon argued that leg force production limits human turning performance during maximum-effort curve running. Based on the assumption that the ability to generate force constrains turning performance, they presented a model that fits the observed relationship between maximum running speed and curve radius (Greene, 1985; Greene, 1987). Maximum speed decreases may primarily be due to limitations of force generation capabilities of the inside leg (Chang et al., 2001; Rand and Ohtsuki, 2000). However, leg force production does not appear to constrain performance for other animals such as greyhounds (Usherwood and Wilson, 2005).

By artificially increasing yaw inertia, body shape was shown to limit maximum turning performance (Carrier et al., 2001). Moreover, during sidestep (using the leg contralateral to the turn direction) and crossover (using the leg ipsilateral to the turn direction) cutting maneuvers, Jindrich et al. argued that for humans, body shape constrains leg forces during sub-maximal speed turns (Jindrich et al., 2006). Specifically, they hypothesized that the braking forces observed during walking and running turns are required to prevent over-rotation about the vertical axis, and presented a simple algebraic model capable of predicting ground reaction forces in several conditions. A variant of this model was also successful in describing leg force directions used by cockroaches during turning maneuvers (Jindrich and Full, 1999). However, humans are not ancestrally cursorial (Schmitt and Lemelin, 2002), and it is unclear whether the constraints on leg forces observed in humans apply to other bipeds. Specifically, it is unclear whether braking forces are required for bipeds of different body shape. Ostriches *Struthio camelus* Linnaeus are cursorial bipeds that depend on running to escape predation, and would be expected to be highly maneuverable. Consequently, ostriches represent an ideal species with which to test this

question and better understand the mechanics of high-performance bipedal maneuverability.

Ostriches could use several possible strategies for achieving the mechanical requirements of changing the movement direction of the center of mass (COM) (deflection) and rotating the body (rotation) during running turns. For example, in turns that take place over multiple strides, cockroaches deflect and rotate in the same stride with body rotation slightly lagging deflection, whereas mice show the opposite pattern where body orientation changes lead deflection (Jindrich and Full, 1999; Walter, 2003). The pattern in mice was attributed to a division of labor where front legs are primarily responsible for rotation and hindlegs responsible for deflection, which also takes advantage of the lower rotational inertia of the body at forelimb-to-hindlimb step transitions. Similar differences among limb girdles are observed in some primate species (Demes et al., 2006). Other such divisions of labor, such as preferentially using one leg to turn, are also possible. For example, bipeds could preferentially use sidesteps or crossover cuts.

In addition to the potential for different behavioral maneuvering strategies there are also many potential motor strategies that could be employed. Maneuvers could result from substantial changes in muscle force and joint torque at one or few joints, or alternatively from strategies that involve modulation and coordination of torque production at many joints. During smooth curve walking, for example, humans turn by modulating coordination patterns observed during straight walking (Courtine and Schieppati, 2004).

The goals of this study were to understand the behavioral and control strategies used by ostriches to turn within the context of the mechanical constraints on legged maneuvers. To this end, we tested the following hypotheses: (1) during anticipated turns, ostriches deflect the trajectory of their COM and rotate their body in the same step; (2) similar to humans, ostriches modulate body rotation during running turns by generating braking forces; (3) turning requires substantial modulation of joint kinematics and torque production for all leg degrees of freedom.

To test these hypotheses, we measured ground reaction forces and joint kinematics while ostriches executed running turns. We measured acceleration/braking forces and compared them to the predictions of a simple turning model to evaluate whether ostriches use these forces to prevent under- or over-rotation as humans do (Jindrich et al., 2006). To evaluate the control strategies employed, we used a quasi-static method to estimate net joint torques during turning and compared them to straight running trials.

Materials and methods

Eight juvenile ostriches *Struthio camelus* L. (mass=22±5 kg, mean ± s.d., range 16–30 kg) were used in the study. The animals were hand-reared from the age of 1 week, and all treatment and experimental procedures were approved by the animal care and use committee at the Royal Veterinary College.

The ostriches were trained to run along a 23 m rubber trackway with a force platform (model 9287BA, Kistler Instrumente AG, Winterthur, Switzerland) embedded mid-way along the length. Metal fencing constrained the running direction to an approximately 1 m corridor, and prevented turning before the force platform. To elicit turning maneuvers, the area enclosed by the metal fencing immediately around the force platform was enlarged, and a large (approximately 1 m^3) cardboard box placed on the trackway behind the platform (Fig. 1A). When confronted with the box, the ostriches executed either sidestep or crossover cuts to the left, which were followed by immediate turns to the right (not analyzed) as the animals continued running around the box. Trials where at least one foot was entirely in contact with the force platform during the stance period were selected for analysis. Following the turning trials, the box barrier was removed, and all animals were induced to run down the same trackway, but not to turn. Depending on whether the ostrich contacted the force platform with the left or right leg, and whether the animal executed a straight run or turn, we grouped trials under four conditions: straight running with the left (SL) and right (SR) legs, crossover turns with the left leg (TL), and sidestep turns with the right leg (TR).

The three-dimensional positions of 13 retroreflective markers attached to the body were measured at 240 Hz using an eight-camera motion tracking system (ProReflex Motion Capture, Qualysis, Inc., Gothenburg, Sweden). Five markers were attached to the body, one above the sacral spine, two on the left and right breast, respectively, and two lateral to each hip joint center (Fig. 1B). For the body markers, small areas of feathers were cut away and the markers attached to the skin, improving marker placement consistency from day to day. Four additional markers were placed on each leg lateral to the knee, ankle and metatarsal-phalangeal (MTP) joints, and one marker was placed on the dorsal skin above the distal interphalangeal joint of the first phalanx (Toe). Kinematic data from body and joint markers were filtered using a fourth-order low-pass Butterworth filter with a cut-off frequency of 20 Hz.

A coordinate frame for the body was established using the five fixed points on the body: the spine, hip and breast points. During some periods of some trials, one or more body points would become obscured from enough camera views to prevent tracking. As long as three of the five body points were tracked, the positions of the remaining missing points were reconstructed based on the three or more visible points and spatial relationships among the body points established during periods when at least four points (the three tracked points and the missing points) were simultaneously visible.

The position of the COM relative to the body points was established for each animal by measuring center of pressure (COP) location when the animal was standing quietly on the force platform, and using the method of zero crossing (Lafond et al., 2004; Zatsiorsky and King, 1998). Given the COM location, the moment of inertia (I) of the animals about the vertical axis could be determined by enticing the animals to execute a nearly stationary turn on the force platform, tracking the COM motion and body rotation, and solving for I using the equations of motion for a rigid body, the known mass (M), linear

and rotational accelerations (Lee et al., 2001). I for ostriches was found to be linearly correlated to $M^{5/3}$, as predicted for geometrically similar bodies (Jindrich and Full, 1999). A least-squares linear fit using M and I values for all animals yielded I=0.0025$M^{5/3}$–0.039, r^2=0.85. For more robust estimates of I, we used this relationship to calculate I from M for each animal.

The global kinematic frame of reference determined by the motion tracking system calibration had a vertical Z-axis, the X-axis approximately aligned with the trackway (and thus approximately aligned with the direction of motion of the animals during straight runs or prior to turning), and the positive Y-axis pointing left in the direction that the animals turned. For each sampled timestep of each trial, the instantaneous COM position was calculated from the body markers. COM positions were then differentiated with respect to time using a fourth-order difference equation, yielding COM velocity. For each step, the initial movement direction (*imd*) was determined from the instantaneous COM velocity at the beginning of stance. A coordinate frame was established with one axis vertical, one coincident with the projection of the *imd* on the horizontal plane, and the third axis orthogonal to these axes. Kinematic and force data were then expressed in this coordinate frame.

To test whether forces in the *imd* were used to control body rotation, we used a simple, two-dimensional mathematical model that can predict the ground reaction forces necessary to maintain body rotation aligned with movement deflection based on few, easily measured parameters (Jindrich et al., 2006; Jindrich and Full, 1999). The model assumes that a biped traveling with velocity V, seeks to deflect the direction of movement by θ_d during a step. At the beginning of the step, the foot is placed at an anterior extreme position ($P_{AEP,imd}$) with respect to the COM parallel to the initial movement direction, and generates a sinusoidal lateral force for the duration of stance. If the foot does not remain directly lateral to the COM, generating the lateral impulse necessary to change the movement direction will result in a torque that rotates the body by θ_p. The proportion that body rotation caused by $F_p(t)$ matches movement deflection can be estimated by a 'leg effectiveness number', an indication of the degree to which maneuvers that maintain body orientation aligned with movement deflection can be achieved simply by generating the forces perpendicular to the movement direction necessary for deflection. The leg effectiveness ϵ can be calculated using a simple algebraic equation based on behavioral and morphological parameters:

$$\epsilon = \frac{\theta_p}{\theta_d} = \frac{MV\tau}{2I}\left(P_{AEP,imd} - \frac{4V\tau}{\pi^2}\right), \quad (1)$$

where τ is the stance period. Values of ϵ close to 1 represent conditions where little modulation of *imd* forces is required for body rotation to match movement deflection at the end of the turn. In the case where *imd* forces are required, their magnitude can be predicted using the equation:

$$F_{imd,max} = \frac{\pi I(1-\epsilon)\theta_d}{\tau^2 P_p}, \quad (2)$$

where P_p is the foot placement perpendicular to the *imd*. A more complete description and derivation of these equations is given elsewhere (Jindrich et al., 2006).

Stance onset and offset were identified as when vertical

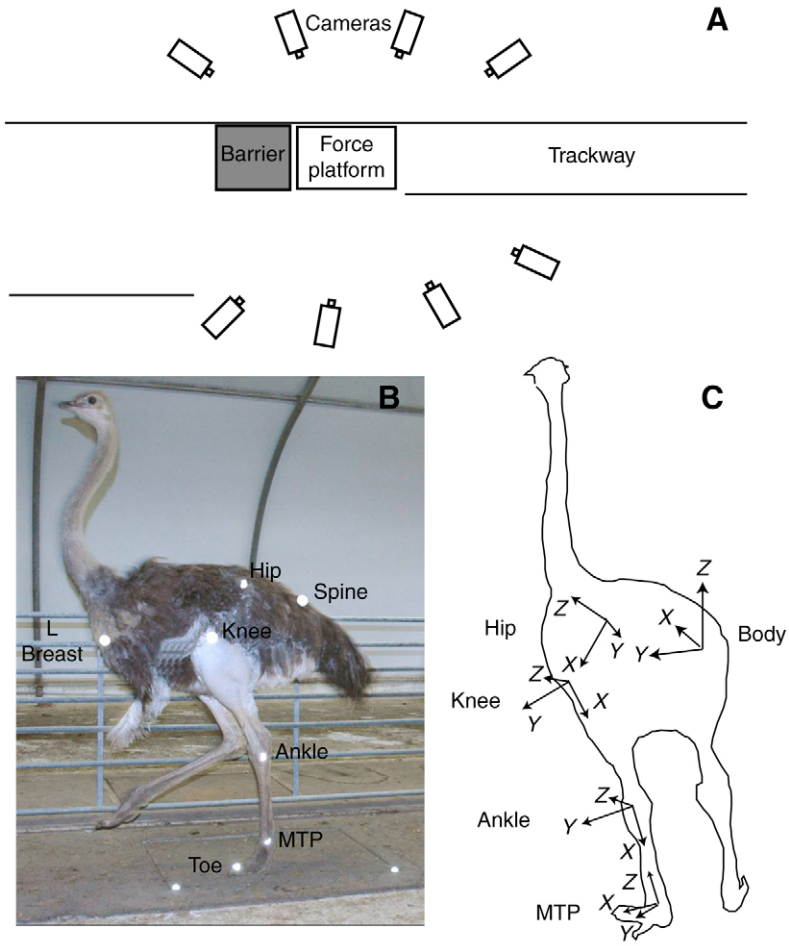

Fig. 1. Experimental setup. (A) Plan view schematic of experimental arena. Ostriches ran along a narrow trackway until encountering a barrier placed directly beyond a force platform. Turns where ostriches stepped on the force platform were recorded and analyzed. Three-dimensional positions of 13 points on the body and legs were measured with a camera-based motion analysis system. (B) Points placed on the left side of an ostrich (with the exception of Spine, equivalent points were placed on the right side). Points were placed near joint centers for the hip, knee, ankle and MTP. (C) Angle convention used to analyze kinematic data. The X-axis was aligned axially along the fore–aft axis of the body and along leg segments. The Y-axis was approximately normal to the plane of motion of the joint. The Z-axis was normal to the X and Y axes. The two ground points identified the force platform in the tracking system but were not used for analysis.

Table 1. *Parameters measured during four experimental conditions*

Condition	Straight left (SL)	Straight right (SR)	Crossover (TL)	Sidestep (TR)
N	40	42	56	63
Deflection, θ_d (deg.)	–0.1±0.7	0.8±0.7	14.1 ± 0.6^{SL}	$18.0\pm0.6^{SR,TL}$
Initial body angle relative to trackway (deg.)	5±1	-1 ± 1^{SL}	$10\pm1^{SR,SL}$	$4\pm1^{SL,SR,TL}$
Initial body angle relative to *imd* (deg.)	6±1	-1 ± 1^{SL}	$11\pm1^{SR,SL}$	$5\pm1^{SR,TL}$
Body angle change, θ_r (deg.)	–4±1	6 ± 1^{SL}	5 ± 1^{SL}	$19\pm1^{SL,SR,TL}$
Initial rotational velocity $\dot{\theta}_i$ (deg. s^{-1})	–9±4	18 ± 4^{SL}	14 ± 4^{SL}	$31\pm4^{SL,SR,TL}$
Body angle relative to *imd* at end of step (deg.)	–1±1	5 ± 1^{SL}	$16\pm1^{SL,SR}$	$23\pm1^{SL,SR,TL}$
Initial transverse leg angle (deg.)	8±1	-3 ± 1^{SL}	$24\pm1^{SL,SR}$	$14\pm1^{SL,SR,TL}$
Transverse force angle (deg.)	0±1	1±1	$14\pm1^{SL,SR}$	$15\pm1^{SL,SR}$
COM vertical position (m)	0.76±0/02	0.76±0.02	$0.72\pm0.02^{SL,SR}$	$0.72\pm0.02^{SL,SR}$
Maximum resultant force (N)	505±32	534±32	$463\pm32^{SL,SR}$	$439\pm31^{SL,SR}$
Maximum vertical force (N)	503±31	522±31	$447\pm31^{SL,SR}$	$417\pm31^{SL,SR,TL}$
Full-sine component fitted to *imd* force (N)	46.5±4.2	48.5±4.2	$41.4\pm4.2^{SL,SR}$	42.6 ± 4.2^{SR}
Acceleratory or braking force in the *imd*, β (N)	–0.5±4.3	3.2±4.2	–5.4±4.0	$-12.0\pm3.8^{SL,SR}$
Maximum fitted perpendicular force, F_{pmax} (N)	–1.4±6.1	10.7±6.0	$96.2\pm5.6^{SL,SR}$	$113.0\pm5.4^{SL,SR,TL}$
Perpendicular force impulse (N s)	–0.2±1.0	1.3±1.0	$14.0\pm1.0^{SL,SR}$	$17.0\pm0.9^{SL,SR,TL}$
Net torque impulse (Nm s)	0.01±0.08	–0.01±0.08	$0.47\pm0.08^{SL,SR}$	$0.42\pm0.08^{SL,SR}$
Body rotation from forces θ_r^{wb} (deg.)	0±1	–2±1	11±1	9±1
Body rotation from forces without braking/acceleration θ_r^{wob} (deg.)	0±2	–3±2	$11\pm2^{SL,SR}$	$18\pm2^{SL,SR,TL}$
Initial velocity, V_i (m s^{-1})	3.3±0.2	3.4±0.2	$2.7\pm0.2^{SL,SR}$	$2.6\pm0.1^{SL,SR}$
Final velocity (m s^{-1})	3.2±0.2	3.4±0.1	$2.7\pm0.2^{SL,SR}$	$2.6\pm0.1^{SL,SR}$
Stance period, τ (s)	0.19±0.01	0.18±0.01	$0.22\pm0.01^{SL,SR}$	$0.22\pm0.01^{SL,SR}$
Initial foot placement in *imd*, $P_{AEP,imd}$ (m)	0.25±0.01	0.26±0.01	0.29 ± 0.01^{SL}	$0.31\pm0.01^{SL,SR,TL}$
Initial foot placement perpendicular to *imd* $P_{AEP,ip}$ (m)	0.01±0.01	–0.03±0.01	$-0.18\pm0.01^{SL,SR}$	$-0.21\pm0.01^{SL,SR,TL}$
Leg effectiveness, ϵ	0.2±0.1	0.3±0.1	$0.9\pm0.1^{SL,SR}$	$1.2\pm0.1^{SL,SR,TL}$

Values are means ± s.e.m. Significant differences among conditions are indicated by superscripts.
imd, direction of initial movement.

forces (F_v) exceeded or dropped below 5% of the maximum forces of the trial, respectively. For some steps (typically the second step of a trial), the foot only partially contacted the force platform. Consequently, if the maximum F_v of an identified stance period did not exceed 75% of the maximum F_v for the entire trial, the step was discarded. In addition, some steps showed a 'toe' region where low forces were maintained, and the maximum F_v did not occur at mid-stance. Consequently, for calculating τ and $P_{AEP,imd}$ for Eqn 1 and Eqn 2, stance onset and offset were normalized to center the maximum F_v at mid-stride. On average, τ decreased by 3% and $P_{AEP,imd}$ decreased by 6%.

To characterize the motions of the body and legs, we assumed that the body had 6 degrees of freedom (d.f.) and that the legs could be characterized using five primary rotational d.f. Motions of the body relative to the global coordinate system were described using Euler angles in the order *Z*-*X*-*Y*. Rotation about *Z* (yaw) and *Y* (pitch) were calculated from the vectors connecting the spine and mid-breast and mid-hip points, respectively. Rotation about *X* (roll) was calculated from the hip points.

We modeled the legs as a chain of rigid segments using the points placed over the joint centers. The orientation of the first segment (the femur) was expressed relative to the body using Euler angles in the order *Y* then *Z*, to align the *X*-axis along the long axis of the femur. The *Y* angle corresponds to flexion/extension, and the *Z* angle approximates ab/adduction of the hip joint relative to the body, although the correspondence between Euler angles and common clinical definitions of rotations is not exact (Wu et al., 2002; Wu et al., 2005). Each successive segment was related to the proximal segment using Euler angles in the order *Z* then *Y*. *Z*-rotation approximates ab/adduction of the distal segment, and *Y*-rotations approximate flexion–extension of the joint (Fig. 1C). These calculations do not account for potential axial rotations about segmental *X*-axes.

Forces and moments were transformed into the kinematic coordinate system using an empirical calibration derived from measurements of COP location in the force platform coordinate frame [corrected according to the method described elsewhere (Bobbert and Schamhardt, 1990)], using a known weight with position measured using the motion tracking system. The free moment was calculated using the forces and moments measured by the force platform (Holden and Cavanagh, 1991). Due to the inability to fully account for axial (*X*) rotations using the marker set employed, complete inverse-dynamics calculations of joint torques were not possible. Consequently, quasi-static joint torques (that do not account for segmental inertias) were calculated from the endpoint forces and moments and leg configuration angles using an iterative Newton–Euler algorithm (Craig, 1989). Quasi-static torques for each joint were expressed in the coordinate system of the distal segment of the joint (McLean et al., 2005): T_y represents flexion/extension torque, T_z varus/valgus torque, and T_x rotational torque about the segment axis. Torque impulse for each d.f. was calculated by

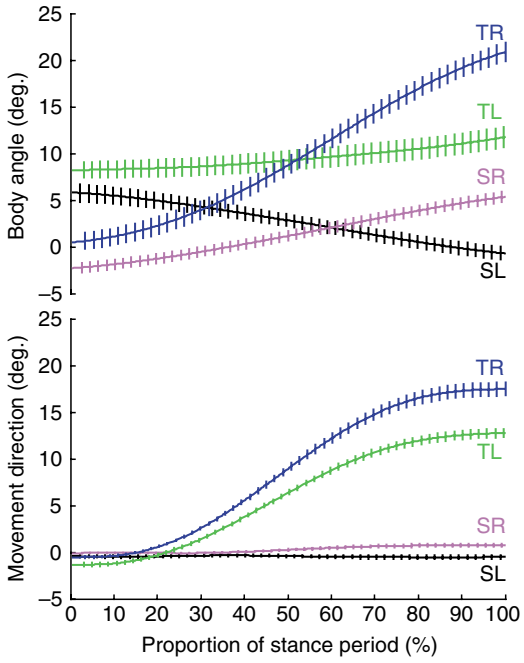

Fig. 2. Body rotation and deflection of the COM during the stance period of four conditions, straight running steps with the right (SR; magenta line) and left (SL; black line) legs, sidesteps with the right leg (TR; blue line) and crossovers with the left leg (TL; green line). Both angles are expressed in initial movement direction reference frame. Angles were scaled to percentage of the stance period, and averaged. Vertical whiskers denote s.e.m. at each phase of stance.

integrating torque with respect to time. All calculations were performed using custom analysis routines written in MATLAB (The Math Works, Inc., Natick, MA, USA).

To compare kinematic, force and torque data among different trials, data were linearly rescaled to phase of stance, with a resolution of 0.1%, resulting in time series of 1000 points. Scaled force, angle and torque time series from left and right legs during straight steps were averaged to yield reference trajectories for each parameter, degree of freedom, and leg. To statistically compare kinematic time series, the reference trajectories for straight-running trials for each leg were subtracted from the data for each trial corresponding to the same leg, yielding a set of differences from the reference trajectory for each trial. The L-2 norm of the differences was calculated to yield a single 'error' value for each kinematic parameter and trial (Jindrich and Full, 1999).

We statistically compared measured parameters using repeated-measures ANOVA, with animal as the repeated measure and maneuver type (SL, SR, TL and TR) as the main effect. Reported means and standard errors (s.e.m.) represent least-squares means from the ANOVA model. We used the JMP 4.0 (SAS Institute, Inc., Cary, NC, USA) software package for statistical calculations.

Results

Ostriches did not execute sidestep or crossover cuts with frequencies significantly different from 50% (χ^2 test; $P>0.5$), and the observed body angle changes were not significantly different between sidesteps and crossover cuts (Table 1). However, ostriches showed significantly greater movement deflection for sidestep cuts relative to crossovers. The movement deflections of 14° and 18° corresponded to turning radii of 2.4 m for crossovers and 1.8 m for sidesteps, respectively.

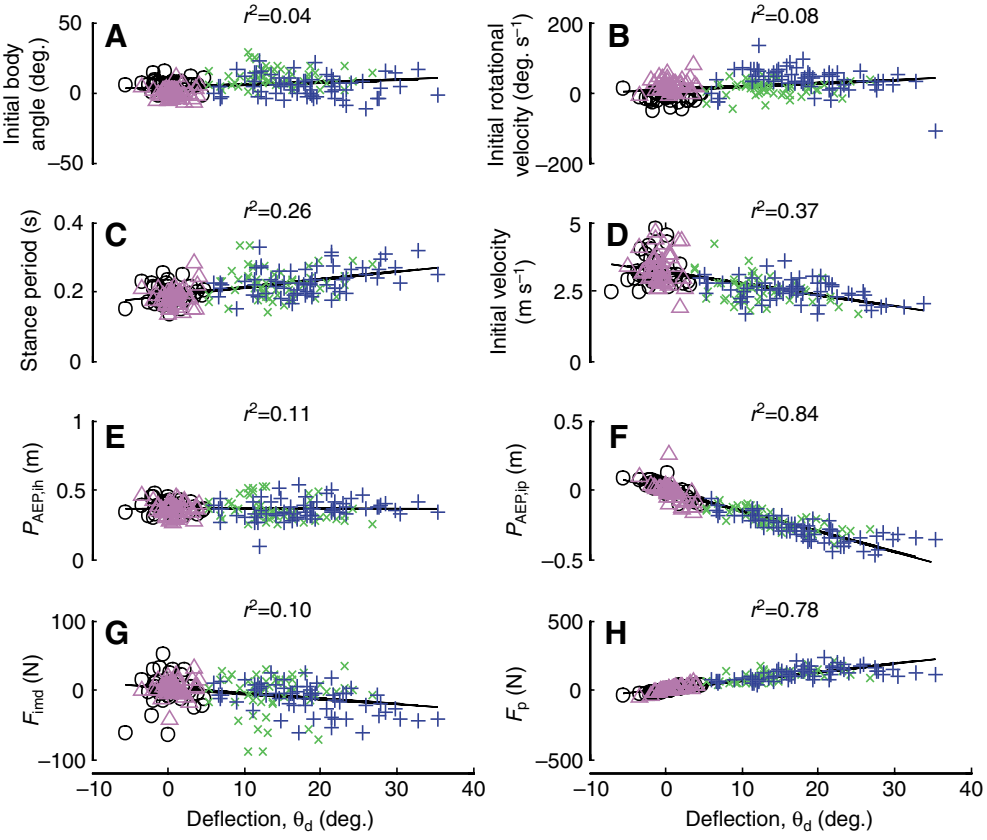

Fig. 3. Relationships between turn magnitude (deflection; θ_d) kinematic and force parameters important for turning. All four conditions are shown: straight running steps with the right (magenta triangles) and left (black circles) legs, sidesteps with the right leg (blue plus signs) and crossovers with the left leg (green crosses). Linear relationships from least-squares fits are indicated by black lines, and r^2 values indicated for each relationship.

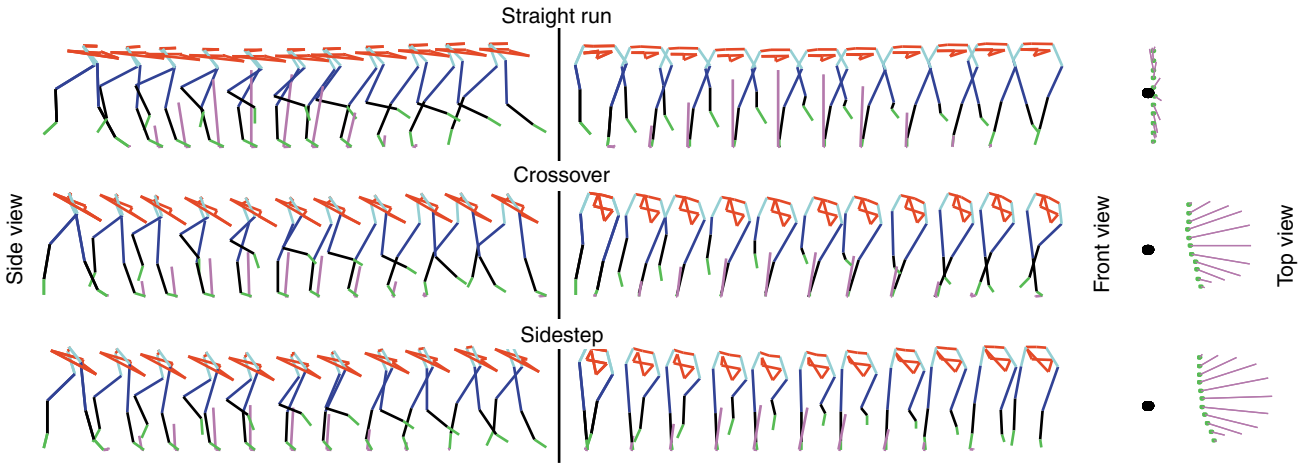

Fig. 4. Stick figure representation of representative (i.e. trials with deflections closest to mean deflection for each turn type) trials for three types of running turns. Magenta line denotes force vector (of arbitrary scale for visualization). In Top View representation, only COM (black circle) and foot (green point) are shown, and magenta line denotes average forces for all trials in the indicated turn condition.

During sidesteps, ostriches deflect the trajectory of their COM and rotate their body in the same step. Ostriches overcome normal body rotation during crossovers

Ostriches anticipated turns with changes in body orientation and rotational velocity. Initial body angles relative to the trackway and *imd* for sidesteps were significantly different from both straight runs with the same leg and crossover cuts (Table 1). However, these differences in body orientation were small relative to the changes in body angle achieved during the subsequent step. The initial body angle before sidesteps was 6° higher than for straight steps of the same leg, compared to changes in body angle of almost 20° for sidesteps. Over 90% of the body rotation during sidesteps occurred during steps where movement direction was deflected. Sidesteps therefore involved simultaneous changes in movement direction and body orientation.

Crossover cuts, however, showed less absolute body rotation, and rotation was not closely associated with movement deflection (Fig. 2). Rotation during crossover steps only accounted for one-third of the total body rotation, with increased initial body rotation accounting for the remainder. However, relative to straight running steps with the same leg ostriches

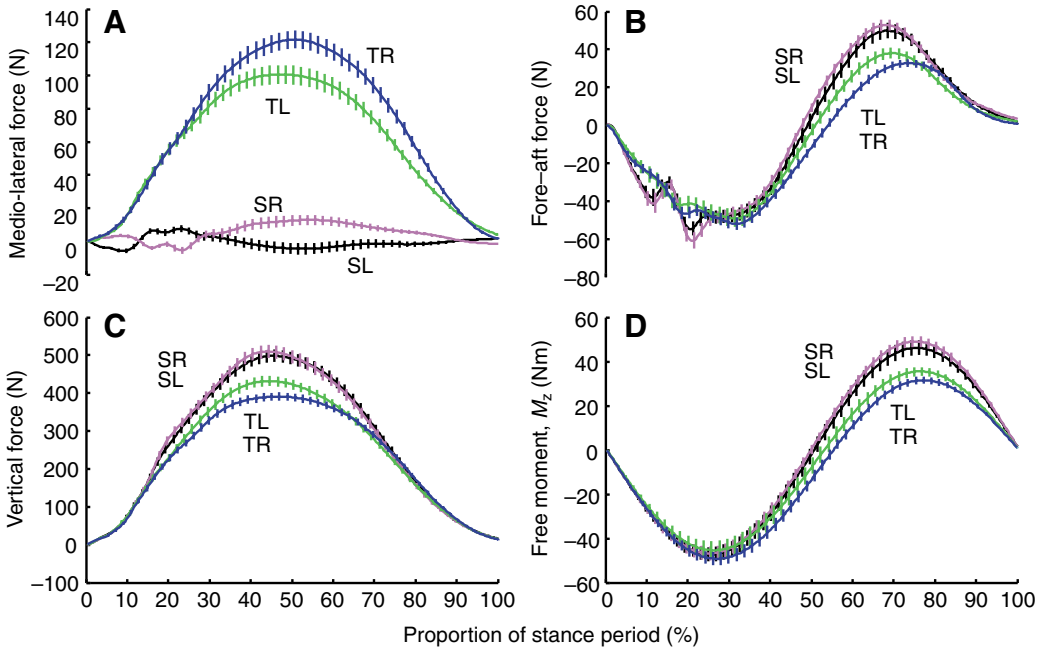

Fig. 5. Forces and free moments for four different conditions. Colors, labels and error bars as described in Fig. 2.

Table 2. *Joint angles at the beginning of steps for four experimental conditions*

Degrees of freedom (d.f.)	Initial angle (deg.)			
	Straight left (SL)	Straight right (SR)	Crossover (TL)	Sidestep (TR)
Body				
Z (yaw)	6±1	–1±1	11±1*	5±1*
X (roll)	2±1	–2±1	–5±1*	–9±1*
Y (pitch)	3±2	3±2	3±2	2±2
Hip				
Y (extension)	51±2	45±2	53±2	43±2
Z (ad/abduction)	21±1	–18±1	20±1	–18±1
Knee				
Z (ad/abduction)	–40±1	40±1	–44±1*	34±1*
Y (flexion)	27±2	35±2	26±2	37±2
Ankle				
Z (ad/abduction)	9±1	–6±1	9±1	–6±1
Y (extension)	–18±1	–18±1	–18±1	–19±1
MTP				
Z (ad/abduction)	5±2	–6±1	4±1	–2±1*
Y (extension)	–29±1	–28±1	–30±1	–30±1

Values are least-squared means ± s.e.m. Asterisks indicate significant differences between values for the same leg during turning relative to straight running.

showed comparable anticipation of turns: 6° and 5° increases in body angle and 13°s^{-1} and 23°s^{-1} in rotational velocity for sidesteps and crossovers, respectively. Consequently, the increased initial body rotation observed during crossovers was largely due to the body orientation during steps of the left leg. Although the body orientation changes during crossovers were less pronounced ostriches simultaneously deflected the body and overcame changes on body orientation that normally occur during steps with the ipsilateral leg.

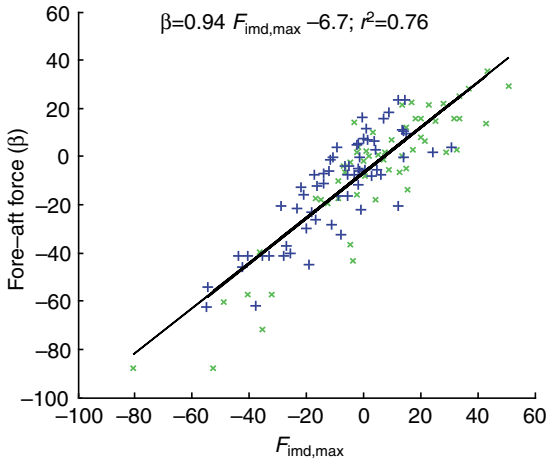

Fig. 6. Comparison of fore–aft forces generated during turning to forces predicted by simple turning model. Sidesteps are plotted as blue plus signs (+), crossovers as green crosses (×).

Turning involved minor changes to kinematics and forces, but few parameters were strongly correlated with turn magnitude

Turn magnitude was associated with lateral shifts in leg placement, but other kinematic parameters did not show strong relationships with turn magnitude, despite significant overall changes for turning trials. Turn magnitude, as indicated by the movement deflection (θ_d) during the final turning step showed weak associations with both initial body angle θ_i and initial body rotational velocity $\dot{\theta}_i$, as indicated by correlation coefficients (r^2) of less than 0.1 (Fig. 3A,B). Stance periods (τ) were 15–20% longer and initial velocity (V_i) 20–25% lower during both sidesteps and crossover cuts, but neither showed strong correlations to θ_d (Table 1; Fig. 3C,D). Anterior extreme foot placement in the movement direction ($P_{AEP,imd}$) showed a significant increase only for sidesteps, but also showed weak correlations with θ_d (Fig. 3E). In contrast, sidesteps and

Table 3. *Joint torque impulse measured during four experimental conditions*

Degrees of freedom (d.f.)		Torque impulse (Nm s)			
		Straight left (SL)	Straight right (SR)	Crossover (TL)	Sidestep (TR)
Hip	*Y* (extension)	0.86±0.35	0.51±0.34	1.33±0.34	1.31±0.34*
	Z (valgus)	3.86±0.27	–3.59±0.25	4.14±0.25	–4.02±0.23
	X (rotation)	2.71±0.26	–3.08±0.24	3.36±0.25	–3.22±0.22
Knee	*Y* (flexion)	–0.76±0.25	–1.09±0.23	0.66±0.24*	–1.66±0.22
	Z (valgus)	8.71±0.54	–8.53±0.50	10.07±0.52	–7.24±0.47
	X (rotation)	–2.23±0.16	2.03±0.15	–2.71±0.15	1.89±0.14
Ankle	*Y* (extension)	5.07±0.67	4.57±0.67	5.91±0.67*	5.27±0.67*
	Z (valgus)	0.67±0.24	–0.89±0.23	1.51±0.23*	0.15±0.22*
	X (rotation)	–0.60±0.06	0.72±0.06	-0.58±0.06	0.74±0.05
MTP	*Y* (extension)	3.39±0.37	3.07±0.37	3.93±0.37*	3.51±0.37*
	Z (valgus)	–1.97±0.22	2.02±0.20	–1.36±0.21	2.27±0.19
	X (rotation)	0.26±0.09	0.11±0.09	0.94±0.09*	0.97±0.09*

Values are least-squared means ± s.e.m. Asterisks indicate significant differences between values for the same leg during turning relative to straight running.

crossover cuts both showed significant lateral and medial shifts, respectively, in foot placement perpendicular to the *imd* (P_{pi}) relative to straight runs (Table 1), and P_{pi} also showed a close correlation with θ_d (Fig. 3F).

Both sidesteps and crossover cuts require substantial increases in forces perpendicular to the initial movement direction (F_p; Fig. 4B, Fig. 5A). Turning involved 10- to nearly 100-fold increases in maximum force in the horizontal plane perpendicular to *imd* (F_{pmax}) and perpendicular force impulse relative to straight running, and 50-fold increases in net torque impulse about the COM (Table 1). Relative to F_p and net torque impulses, changes to vertical forces and free moment about the vertical axis (FM_z) were modest (Fig. 4A, Fig. 5B–D). Differences in FM_z that could contribute to modulating body rotation were also small: body rotation due to FM_z was 0.2±0.4° for sidesteps and 1.7±0.4° for crossovers.

Acceleratory or braking forces control body rotation during running turns

Although the group differences in acceleratory/braking forces in the *imd* among maneuver types were small, ostriches did use forces in the *imd* to control body rotation during turning. Only sidestep cuts showed significant differences in acceleratory/braking forces (β) relative to straight-running steps with the same leg (Table 1). Expected rotations without acceleratory/braking forces (θ_r^{wob}) for sidesteps were twice the body rotation due to total forces (θ_r^{wb}). Crossover cuts did not show significant differences in average β relative to straight runs, and body rotations of 11° without braking forces were not different from the body rotation due to total forces.

Ostriches had average leg 'effectiveness' of 0.9 and 1.2 for crossovers and sidesteps, respectively (Table 1), indicating that on average the forces required for movement deflection should generate appropriate body rotations during turning. However, using Eqn 1 and Eqn 2 to predict the braking forces necessary to prevent over-rotation yielded a strong positive correlation (Fig. 6). The simple turning model based on the assumption that forces in the *imd* are used to modulate body rotation could explain over 70% of the variance in *imd* force used during sidesteps and crossover cuts, supporting the hypothesis that for individual trials, braking forces did prevent under- or over-rotation during running turns. The slope of 0.94 was only slightly below the expected slope of 1 for an isometric relationship. Ostriches generated net braking forces during 52% of all trials and 60% of turning trials. That acceleratory forces were present in 40% of the turning trials is consistent with the hypothesis that ostriches used either braking or acceleratory forces to modulate body rotation when necessary.

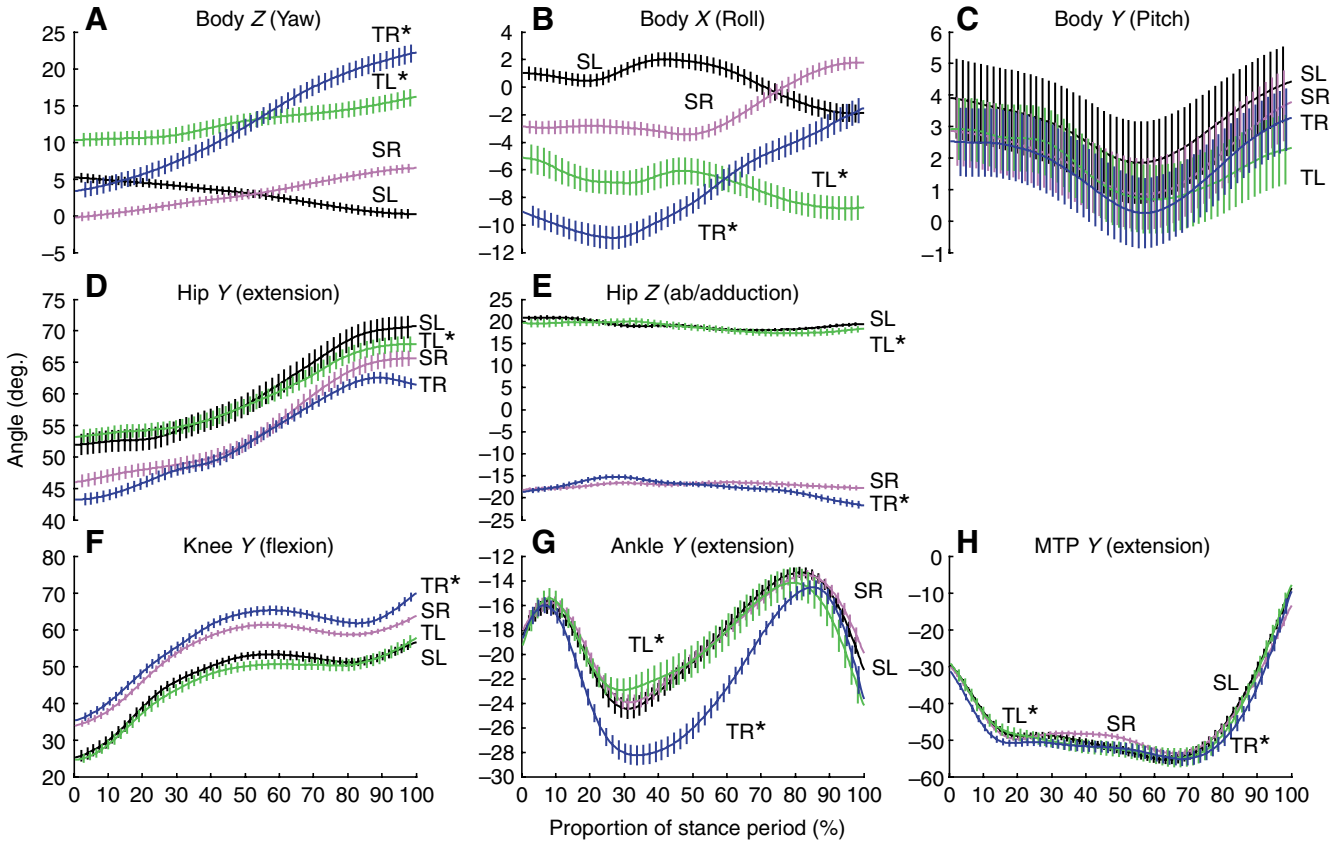

Fig. 7. Body and joint angles during the stance period for four conditions studied. Colors, labels and error bars as described in Fig. 2. Asterisks denote significant differences between kinematics observed during turning and corresponding straight runs with the same legs. MTP, metatarsal–phalangeal.

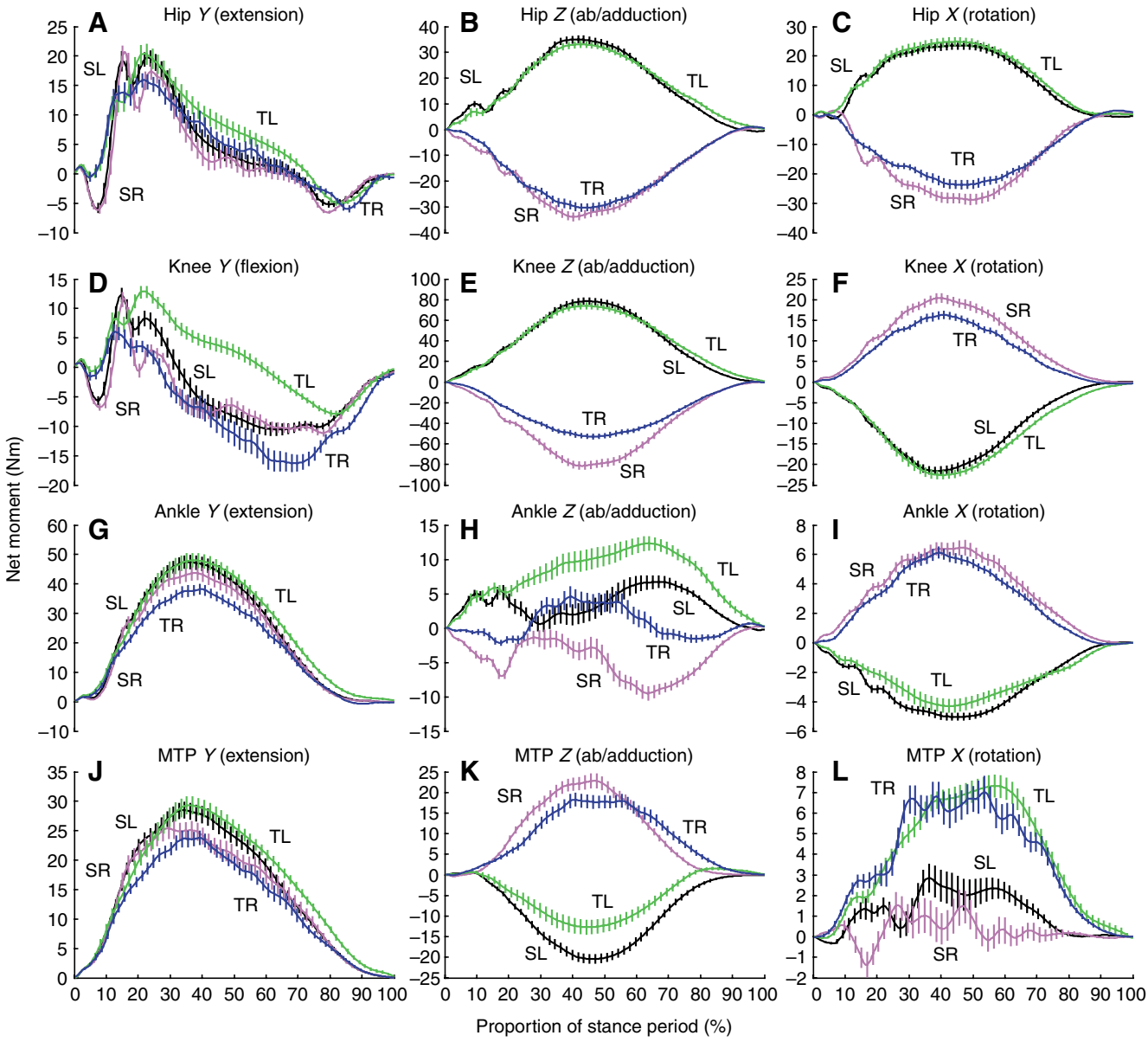

Fig. 8. Net torques about joint axes during the stance period four turning conditions. Colors, labels and error bars as described in Fig. 2. Descriptors in parentheses denote direction of positive angle changes. MTP, metatarsal–phalangeal.

Turning did not require substantial modulation of joint kinematics and torque production

In addition to changes in initial body yaw, ostriches initiated turning steps with significant changes to body roll (Table 2). These changes in roll diminished over the stance period of turning steps for sidesteps, but persisted for crossover cuts (Fig. 7C). However, few changes in initial joint kinematics were observed. The only significant differences in initial joint angles were in knee and MTP *Z*, representing increased adduction at the knee and decreased adduction at the MTP (Table 2).

Significant changes in joint kinematics over the course of turning steps were evident in many joint d.f.s (Fig. 7). However, most of these significant differences were due to increased variability in joint angle trajectories during turning trials. Substantial offsets in joint angle trajectory were only evident in ankle extension during sidesteps.

The substantial increases in F_p during turning did not result in significant alterations of net torque about most joint axes (Table 3; Fig. 8). Only 10 of the 24 joint axes showed significant differences in torque impulse relative to straight runs. The significant increases in axial (*X*) MTP torque impulses were consistent with significant shifts in the COP relative to the toe of 6 cm medially for sidesteps and 5 cm laterally for crossovers. Increases in MTP *X*-axis torque impulses represented less than 25% of the total torque impulse experienced by the joint. Ankle extensor (*Y*) impulses showed significant increases for both sidesteps and crossovers, but the

increases were only 17% and 15% for crossovers and sidesteps, respectively. Although turning also resulted in changes in loading about the ankle *Z*-axis, the absolute changes of 0.84 and 1.04 Nm s were less than 20% of the total torque impulses experienced by the joint. Similar to the ankle, crossover cuts were associated with significantly greater flexor torques at the knee. The knee flexion torques pass through zero, resulting in small net torque impulses during straight-ahead locomotion. Although the increased knee flexor torque impulses during crossovers were twofold those during straight running, the absolute magnitude of the impulses only increased by 10%. Similarly, hip extensor torques during sidesteps also increased over twofold relative to straight-ahead running, but the absolute torque increase was only 44%. Overall, although significant changes in net joint torque impulse were observed, for most joints these changes were small relative to the net torque impulses experienced at each joint.

Discussion

Ostriches did not show a preference for sidesteps or crossovers. During sidesteps, ostriches deflected their movement direction and rotated their body in the same step. During crossovers ostriches primarily changed their movement direction but little body rotation occurred. However, both sidesteps and crossovers showed comparable changes in body orientation relative to straight running and both showed similar anticipatory adjustments in body rotation at the beginning of the step. Leg effectiveness numbers were within 20% of 1, indicating that only small acceleration/braking forces on average should be necessary to control body rotation during turning. As predicted, measured acceleration/braking forces were small in magnitude relative to vertical forces and the forces parallel or perpendicular to the initial movement direction. However, during individual trials ostriches did use acceleration/braking forces to control body orientation during running turns. The measured forces matched the forces predicted to maintain body orientation aligned with movement direction at the end of the turn. The adjustments to foot placement employed were primarily achieved by changes in body attitude and abduction of the shank. Despite the large changes in direction and ground reaction forces necessary to maneuver, large changes in joint torques were not observed.

Several experimental limitations should be taken into account when interpreting these results. First, due to the structure of the trackway, barrier and motion analysis system the trials could not be randomized. Straight running trials were collected beginning 1 day following data collection from turning trials. This non-random presentation of straight runs may have contributed to the observed asymmetry of some kinematic and dynamic parameters (i.e. Fig. 7). Moreover, the environment around the trackway was not symmetrical, and the presence of computers and experimenters to the left of the force platform could also have contributed to the observed asymmetries. Variability in marker placement was also a source of measurement noise. For example, markers on the breast could move dorso-ventrally relative to the other body markers with each breath. Although these motions could change the calculated COM location vertically, we expect that the fore–aft and medio-lateral noise due to respiration to be small. Finally, in these experiments we elicited turns of modest magnitude, and ostriches can certainly execute turns sharper than the 14–18° turns we studied. Consequently, our findings do not exclude the possibility that ostriches use different strategies during turns of very different magnitudes or speeds.

The three-dimensional nature of maneuvers requires a consideration of the three-dimensional movements of the body and limbs. To completely characterize the position or motion of a limb, the segmental (i.e. bone) orientations should be measured and related to each other using consistent angle conventions (Grood and Suntay, 1983; Wu et al., 2002). Determining bone orientations, however, requires multiple markers on each segment, and was not possible in this study. Consequently, we chose to affix markers to landmarks near each joint center, and characterize joint motion using an angle convention that captures the most important features of movement. However, this characterization was not complete, and some potential types of movement (such as axial rotation of the segments), could not be uniquely identified. Moreover, the nature of our kinematic characterization prevented inverse-dynamic calculations of joint torques that would account for the contributions of segmental acceleration to ground reaction forces. However, the impact of these limitations is reduced by the repeated-measures experimental design, and the small differences in joint kinematics observed among the four conditions.

Although ostriches did not change their stride to preferentially turn with one leg, the kinematics of executing crossovers and sidesteps were different. The greater initial body rotation, and reduced rotation observed during crossovers, suggest that body rotation is limited. One reason for reduced rotation during crossovers is the lower leg effectiveness of the inside leg relative to the outside leg (Table 1). However, with a leg effectiveness of 0.9, the body rotation caused by F_p would be expected to be 90% of the deflection magnitude, instead of 36%. This difference is likely caused by other mechanical factors such as the inertia of the swing leg. During straight running steps with the left leg, the body rotated on average –4° (i.e. clockwise; Table 1). The same mechanical factors are likely to constrain rotation during crossovers. Relative to straight steps with the left leg, body angles changed 10° during crossovers, or 83% of the measured deflection. The remaining discrepancy may be due to the need to swing the right leg in the turn direction (medially) for correct placement in the subsequent step, similar to the effects of swing-leg inertia suggested in studies of human maneuvering (Jindrich et al., 2006). For crossovers, the body rotation due to this medial movement would act against the turn direction, and could contribute to the reduced body rotation during turning steps. The similarity of net torque impulses about the COM during sidesteps and crossovers supports the possibility that swing-leg inertia reduces body rotation during crossovers. Although ostriches generated forces appropriate for body rotation to match movement deflection during crossovers,

body rotation during turning was likely reduced by swing-leg inertia. Ostriches appeared to compensate for this limitation by beginning crossovers with increased initial body yaw into the turning direction.

Ostrich morphology is appropriate for effective maneuvers

When humans execute 30° sidestep and crossover cuts, braking forces are 26% of F_{pmax} compared to 6–11% for ostriches executing 15–20° turns (Jindrich et al., 2006). Moreover, whereas humans generated almost exclusively braking forces during sidesteps and crossovers, 40% of the net forces observed during turns for ostriches were acceleratory. Although both ostriches and humans used braking/acceleration forces to control body rotation, this required almost exclusively braking forces by humans. This can be explained in part by differences in leg effectiveness. Whereas humans turn with ϵ=2.0–2.5, ostriches operated at ϵ of approximately half these values, 0.9–1.2 (close to 1). Differences in body shape can account for some of the differences observed between ostriches and humans. In contrast to the orthograde posture of humans, ostriches have a pronograde (i.e. more horizontal than vertical) trunk orientation that results in a larger moment of inertia about the vertical axis. The relationship *M*/*I* for ostriches was 86% of that for humans, and an ostrich-shaped human would be expected to have ϵ=1.2. However, ϵ is most sensitive to the relationship of $P_{AEP,imd}$ to τ and V_i (i.e. the multiplicand of Eqn 1). The fore–aft foot placement ($P_{AEP,imd}$) for ostriches was below (76–79%) those used by humans, but this was almost completely offset by decreases in τ (ostriches 81–85% of humans), and V_i (ostriches 87–93% of humans). The multiplicand of Eqn 1 for ostriches was 95% of human values. Consequently, most of the differences between ostriches and humans were explained by differences in body morphology. Ostrich morphology is appropriate for effective maneuvers that require minimal acceleratory or braking forces.

Turns could be executed with minimal changes in leg kinematics or joint torque production

Ostriches did not substantially alter body or leg kinematics to turn, and the kinematic changes resulted in few alterations to joint torques relative to straight-ahead runnning. The lateral shifts in foot placement relative to the COM ($P_{AEP,ip}$; Table 1) were caused by increased body roll and increased knee adduction and abduction for crossovers and sidesteps, respectively (Table 2). Considering the height of the COM of 76 cm, an initial body roll of 9° would be expected to result in a change in $P_{AEP,ip}$ of 12 cm in the absence of joint angle changes, approximately 60% of the observed shift for sidesteps. For crossovers, body roll alone without changes in leg kinematics would be expected to account for 37% of the $P_{AEP,ip}$ shift. The remainder of $P_{AEP,ip}$ shift can be accounted for by *Z* rotation at the knee: increased adduction during crossovers and abduction during sidesteps, which both serve to shift the foot position towards the outside of the turn. This rotation is most likely due to axial thigh rotation, but varus/valgus movements at the knee could also have contributed to the observed *Z*-rotation. These observed adjustments at the knee joint are similar to changes in knee angles observed by guinea fowl running over rough terrain (Daley and Biewener, 2006). The only other significant change in initial angle, MTP *Z*, contributed to the medial shift in $P_{AEP,ip}$ during crossovers, but was small in magnitude and could not account for substantial shifts in foot position given the length of the foot.

Body roll and leg ab/adduction resulted in transverse leg angles (the angle of the line connecting the toe and hip) that paralleled changes in transverse force angle during turns (Table 1). Transverse leg angle increased by 16° during crossovers and 17° during sidesteps, compared to 14° changes in force angle. Although medio-lateral shifts in the COP resulted in increased *X* and *Z* torques at the MTP and ankle joints, the alignment of the leg and force angles prevented significant increases in *X* and *Z* torque impulses at the knee and hip. Surprisingly, *Y* torques (extension at the ankle and flexion at the knee) increased during crossovers despite a significant decrease in the resultant force (Tables 1, 3). This was most likely due to the increased body yaw at the initiation of the turn during crossovers, which served to increase the component of F_p directed in the positive fore–aft direction, relative to the leg. Patterns of fore–aft and vertical forces relative to the *imd* were maintained during crossovers (Fig. 4), even though this resulted in changes in net torque impulses at distal joints. Overall, considering the large increases in F_p required for turning, changes in joint loading were small: less than 25% with the exception of hip extensor torques during sidesteps. This smooth transition from running to turning is reminiscent of the smooth transition between grounded and aerial running observed in these animals (Rubenson et al., 2004).

These results suggest that, with an appropriately designed morphological system, maneuvers can be executed with minimal changes to running dynamics. Although acceleratory and braking forces did serve to control body rotation, maneuvers did not involve substantial changes to leg kinematics or joint loading. Consequently, these results suggest that maneuvers in ostriches could result from minor modifications of the spring-like behavior of legs during running. Theoretical studies of 'Lateral Leg Springs' have shown that horizontal-plane maneuvers can be executed by spring–mass systems with minor shifts in COP location (Schmitt and Holmes, 2000), a proposition experimentally supported in insects (Jindrich and Full, 1999). These findings parallel theoretical and experimental studies of saggital-plane maneuvers, where the spring-like properties of legs can contribute to energy input in the form of muscle work to result in high performance (McGowan et al., 2005; Seyfarth et al., 1999). Changes in leg placement can contribute to stabilizing movements both through body dynamics and influencing leg stiffness (Farley et al., 1998; Seyfarth et al., 2002; Seyfarth et al., 2003). Additional study is required to determine how musculoskeletal dynamics contributes to satisfying both the translational and rotational stability requirements during three-dimensional maneuvers.

In summary, ostrich morphology is appropriate for maneuvering without requiring large braking or acceleratory

forces. However, ostriches did use forces in the initial movement direction to control body rotation. Ostriches executed maneuvers using a simple control strategy that required minimal changes to leg kinematics or net torque production at individual joints. Body roll and ab/adduction of the leg shifted the foot position away from the turn direction, reducing the braking or acceleration forces required to control body rotation and aligning the leg with the ground reaction force.

List of symbols and abbreviations

COM	center of mass
COP	center of pressure
d.f.	degrees of freedom
FM_z	free moment about the vertical axis
F_p	force in horizontal plane perpendicular to the *imd*
F_{pmax}	maximum force in horizontal plane perpendicular to the *imd*
F_v	vertical force
I	moment of inertia about the vertical axis
imd	initial movement direction
M	body mass
MTP	metatarsal–phalangeal
$P_{AEP,imd}$	anterior extreme foot placement in the initial movement direction
P_p	foot placement perpendicular the *imd*
P_{pi}	initial foot placement perpendicular the *imd*
SL	straight-running step with the left leg
SLIP	spring-loaded inverted pendulum
SR	straight-running step with the right leg
t	time
TL	left turn stepping with the left leg (crossover)
TR	left turn stepping with the right leg (sidestep)
T_x	torque about the *X* segment axis (axial rotation)
T_y	torque about the *Y* segment axis (flexion/extension)
T_z	torque about the *Z* segment axis (varus/valgus)
V	velocity magnitude
V_i	initial velocity magnitude
β	acceleratory or braking force in the *imd*
ϵ	leg effectiveness number
θ_d	angular change in velocity vector (magnitude of deflection)
θ_p	body rotation due to lateral impulse necessary for movement deflection
θ_r^{wb}	expected body rotation with acceleratory or braking forces in the *imd*
θ_r^{wob}	expected body rotation without acceleratory or braking forces in the *imd*
$\dot{\theta}$	initial body angle
$\dot{\theta}_i$	initial body rotational velocity
τ	stance period

The authors acknowledge the BBSRC for funding this work. A.W. is a BBSRC Research Fellow and holder of the Royal Society Wolfson Research Merit award. The authors thank Justine Robillard, Dr Jim Usherwood, Dr Renate Weller (Royal Veterinary College, UK) and Prof. Roger Woledge (Kings College London, UK) for their technical help.

References

Alexander, R. M. (2003). Stability and manoeuvrability of terrestrial vertebrates. *Integr. Comp. Biol.* **42**, 158-164.

Bobbert, M. F. and Schamhardt, H. C. (1990). Accuracy of determining the point of force application with piezoelectric force plates. *J. Biomech.* **23**, 705-710.

Carrier, D. R., Walter, R. M. and Lee, D. V. (2001). Influence of rotational inertia on turning performance of theropod dinosaurs: clues from humans with increased rotational inertia. *J. Exp Biol.* **204**, 3917-3926.

Cavagna, G. A., Heglund, N. C. and Taylor, C. R. (1977). Mechanical work in terrestrial locomotion: two basic mechanisms for minimizing energy expenditure. *Am. J. Physiol.* **233**, R243-R261.

Chang, Y. H. and Kram, R. (2007). Limitations to maximum running speeds on flat curves. *J. Exp. Biol.* **210**, 971-982.

Courtine, G. and Schieppati, M. (2004). Tuning of a basic coordination pattern constructs straight-ahead and curved walking in humans. *J. Neurophysiol.* **91**, 1524-1535.

Craig, J. (1989). *Introduction to Robotics: Mechanics and Control*. Reading, MA: Addison-Wesley.

Daley, M. A. and Biewener, A. A. (2006). Running over rough terrain reveals limb control for intrinsic stability. *Proc. Natl. Acad. Sci. USA* **103**, 15681-15686.

Demes, B., Carlson, K. J. and Franz, T. M. (2006). Cutting corners: the dynamics of turning behaviors in two primate species. *J. Exp. Biol.* **209**, 927-937.

Dickinson, M. H., Farley, C. T., Full, R. J., Koehl, M. A. R., Kram, R. and Lehman, S. (2000). How animals move: an integrative view. *Science* **288**, 100-106.

Farley, C. T. and Morgenroth, D. C. (1999). Leg stiffness primarily depends on ankle stiffness during human hopping. *J. Biomech.* **32**, 267-273.

Farley, C., Glasheen, J. and McMahon, T. A. (1993). Running springs: speed and animal size. *J. Exp. Biol.* **185**, 71-86.

Farley, C. T., Houdijk, H. H., Van Strien, C. and Louie, M. (1998). Mechanism of leg stiffness adjustment for hopping on surfaces of different stiffnesses. *J. Appl. Physiol.* **85**, 1044-1055.

Full, R. J. (1989). Mechanics and energetics of terrestrial locomotion: bipeds to polypeds. In *Energy Transformations in Cells and Organisms. Proceedings of the 10th Conference of the European Society for Comparative Physiology and Biochemistry* (ed. W. Wieser and E. Gnaiger), pp. 175-181. Innsbruck, Stuttgart, New York: Georg Thieme Verlag.

Full, R. J. and Koditschek, D. E. (1999). Templates and anchors: neuromechanical hypotheses of legged locomotion on land. *J. Exp. Biol.* **202**, 3325-3332.

Greene, P. R. (1985). Running on flat turns: experiments, theory, and applications. *J. Biomech. Eng.* **107**, 96-103.

Greene, P. R. (1987). Sprinting with banked turns. *J. Biomech.* **20**, 667-680.

Grood, E. S. and Suntay, W. J. (1983). A joint coordinate system for the clinical description of three-dimensional motions: application to the knee. *J. Biomech. Eng.* **105**, 136-144.

Holden, J. P. and Cavanagh, P. R. (1991). The free moment of ground reaction in distance running and its changes with pronation. *J. Biomech.* **24**, 887-897.

Jindrich, D. L. and Full, R. J. (1999). Many-legged maneuverability: dynamics of turning in hexapods. *J. Exp. Biol.* **202**, 1603-1623.

Jindrich, D. L., Besier, T. F. and Lloyd, D. G. (2006). A hypothesis for the function of braking forces during running turns. *J. Biomech.* **39**, 1611-1620.

Lafond, D., Duarte, M. and Prince, F. (2004). Comparison of three methods to estimate the center of mass during balance assessment. *J. Biomech.* **37**, 1421-1426.

Lee, D. V., Walter, R. M., Deban, S. M. and Carrier, D. R. (2001). Influence of increased rotational inertia on the turning performance of humans. *J. Exp. Biol.* **204**, 3927-3934.

McGowan, C. P., Baudinette, R. V., Usherwood, J. R. and Biewener, A. A. (2005). The mechanics of jumping *versus* steady hopping in yellow-footed rock wallabies. *J. Exp. Biol.* **208**, 2741-2751.

McLean, S. G., Huang, X. and van den Bogert, A. J. (2005). Association

between lower extremity posture at contact and peak knee valgus moment during sidestepping: implications for ACL injury. *Clin. Biomech. Bristol Avon* **20**, 863-870.

Rand, M. K. and Ohtsuki, T. (2000). EMG analysis of lower limb muscles in humans during quick change in running directions. *Gait Posture* **12**, 169-183.

Rubenson, J., Heliams, D. B., Lloyd, D. G. and Fournier, P. A. (2004). Gait selection in the ostrich: mechanical and metabolic characteristics of walking and running with and without an aerial phase. *Proc. Biol. Sci* **271**, 1091-1099.

Schmitt, D. and Lemelin, P. (2002). Origins of primate locomotion: gait mechanics of the woolly opossum. *Am. J. Phys. Anthropol.* **118**, 231-238.

Schmitt, J. and Holmes, P. (2000). Mechanical models for insect locomotion: dynamics and stability in the horizontal plane II. Application. *Biol. Cybern.* **83**, 517-527.

Seyfarth, A., Friedrichs, A., Wank, V. and Blickhan, R. (1999). Dynamics of the long jump. *J. Biomech.* **32**, 1259-1267.

Seyfarth, A., Geyer, H., Günther, M. and Blickhan, R. (2002). A movement criterion for running. *J. Biomech.* **35**, 649-655.

Seyfarth, A., Geyer, H. and Herr, H. (2003). Swing-leg retraction: a simple control model for stable running. *J. Exp. Biol.* **206**, 2547-2555.

Usherwood, J. R. and Wilson, A. M. (2005). Biomechanics: no force limit on greyhound sprint speed. *Nature* **438**, 753-754.

Walter, R. M. (2003). Kinematics of 90 degree running turns in wild mice. *J. Exp Biol.* **206**, 1739-1749.

Wu, G., Siegler, S., Allard, P., Kirtley, C., Leardini, A., Rosenbaum, D., Whittle, M., D'Lima, D. D., Cristofolini, L., Witte, H. et al. (2002). ISB recommendation on definitions of joint coordinate system of various joints for the reporting of human joint motion – part I: ankle, hip, and spine. International Society of Biomechanics. *J. Biomech.* **35**, 543-548.

Wu, G., van der Helm, F. C., Veeger, H. E., Makhsous, M., Van Roy, P., Anglin, C., Nagels, J., Karduna, A. R., McQuade, K., Wang, X. et al. (2005). ISB recommendation on definitions of joint coordinate systems of various joints for the reporting of human joint motion – Part II: shoulder, elbow, wrist and hand. *J. Biomech.* **38**, 981-992.

Zatsiorsky, V. M. and King, D. L. (1998). An algorithm for determining gravity line location from posturographic recordings. *J. Biomech.* **31**, 161-164.